

Study of the diffusion of conservation products in inorganic porous materials combining neutron radiography and vibrational spectroscopy

C. CONTI

Consiglio Nazionale delle Ricerche, Istituto per la Conservazione e la Valorizzazione dei Beni Culturali (ICVBC) - Via Cozzi 53, 20125, Milano, Italy

ricevuto il 28 Gennaio 2014; approvato il 10 Giugno 2014

Summary. — One of the most significant parameters used to evaluate the efficacy of a conservation treatment is the diffusion of the product on the surface and inside the monument porous materials. Though a lot of information has been obtained about the surface, there is a lack of data on the distribution of the organic-polymeric or inorganic-mineral conservation products inside a decayed porous substrate. The aim of this study is to evaluate the effectiveness of neutron radiography and spectroscopic techniques (Raman and FTIR) on the diffusion of ammonium oxalate, an inorganic-mineral conservation treatment, and of three organic-polymeric commercial products widely used in the conservation yards. The results highlighted that the coupling of these techniques turns out to be an effective integrated approach; advantages and drawbacks were evaluated and discussed.

PACS 87.64.km – Infrared.

PACS 87.64.kp – Raman.

PACS 87.57.Va – Neutron imaging; neutron tomography.

1. – Introduction

In recent years, there has been an increasing interest in the study of the conservation treatments diffusion inside the Cultural Heritage matrices. In fact, one of the key factors to define the effectiveness and durability of a treatment is its distribution and penetration. For several years the conservation scientists have been working to find the most suitable methods to evaluate, in a direct way, the diffusion of a treatment in the porous materials [1-7]. Most of them are destructive and they are unable to provide an overview of the treatment diffusion inside the sample in its entirety; the distribution of some organic products was also probed by X-ray microcomputed tomography (micro-CT) [8] and by neutron imaging, an emerging method for Cultural Heritage investigation. Due to the their charge neutrality, neutrons can penetrate thick samples showing hidden details past

TABLE I. – *Treatments of specimens: substrate, product, applied quantities (n.d.: not detectable) and application method.*

Specimen	Substrate	Applied product	Composition	Solvent	Amount of product (mg/cm ²)	Application method
RC	Plaster	Ammonium oxalate	(NH ₄) ₂ C ₂ O ₄	Water	n.d.	Poultice
N1	Stone	Ammonium oxalate	(NH ₄) ₂ C ₂ O ₄	Water	n.d.	Immersion
N2	Stone	Untreated	–	–	–	–
PB	Plaster	Paraloid B72	Ethylmethacrylate/methacrylate	chloroform	14.0	Pipette
MW	Plaster	Mowilith 50	polyvinylacetate homopolymer	chloroform	14.0	Pipette
S1	Plaster	Silres BS290	mixture of silane	2-propanol	66.0	Pipette
S2	Plaster	Silres BS290	and alkylalkoxysilane		14.0	Pipette

outer corrosion and/or buried layers into bulky objects [9-13]. Neutrons interact significantly with light elements, such as hydrogen, giving detectable image contrast. Such a circumstance candidates the neutron imaging as a possible tool to determine the water absorption and distribution inside the material [14-16] and to identify the content and the penetration depth of hydrogen-rich conservation products inside porous stone samples or other materials such as bricks or wood [17-19]. However, the scientific community agrees on the importance of an integrated approach in an attempt to obtain a deeper understanding of the treatment distribution merging the data coming from different analytical techniques.

The aim of this study is to evaluate the effectiveness of the combined application of neutron radiography and vibrational spectroscopy (Raman and FTIR). The diffusion of ammonium oxalate [(NH₄)₂(C₂O₄)], an inorganic-mineral conservation treatment widely used for several years in order to preserve the surfaces of limestones, marbles or plasters, has been studied with μ Raman spectroscopy and neutron radiography. This compound reacts with the calcium carbonate of the substrate to induce the formation of whewellite (CaC₂O₄ · H₂O) and weddellite [CaC₂O₄ · (2 + x)H₂O] [20]. These minerals have got intense and distinguishable Raman lines, especially in the O-C-O stretching range (1400–1500 cm⁻¹), thus μ Raman mapping of whewellite and weddellite allows obtaining the penetration depth of the treatment [6, 7]. Moreover, the presence of hydrogen in the composition of the newly formed minerals supports the hypothesis of a different neutron absorption of the treated portions compared with the untreated ones [17-19]. For this reason, even though neutron radiography has never been applied to probe inorganic products so far, it has been tested here in order to achieve the diffusion overview of ammonium oxalate. Neutron radiography has been used as well to investigate the diffusion of three organic-polymeric commercial products widely used in the conservation yards. The results have been supported by FTIR reflectance measurements, a spectroscopic technique suitable for the analysis of organic-polymeric substances.

2. – Materials

a) An actual painted plaster fragment (1 × 1.5 × 1 cm) from a historical mural painting treated with ammonium oxalate (table I) was analysed by μ Raman spectroscopy in order to map the distribution of calcium oxalate phases.

b) “Noto” stone specimens ($5 \times 5 \times 1 \text{ cm}^3$) were treated in laboratory with ammonium oxalate in order to study its diffusion into the stone by neutron radiography (table I). “Noto” stone is a calcarenite (mainly consisting of calcite [CaCO_3]) employed for a long time as construction material for historical buildings. The specimens were treated by *immersion* in an ammonium oxalate solution 5% w/w in water (24 hours).

c) Plaster specimens ($40 \times 40 \times 10 \text{ mm}^3$) were treated in laboratory (table I) with organic-polymeric conservation products (Paraloid B72, Mowilith 50, Silres BS290) in order to study the diffusion of the treatments by neutron radiography and FTIR spectroscopy. The treatments were performed using a pipette; suitable solutions of the products were deposited on each specimen in multiple steps. The quantities applied for every sample (shown in table I) were in the range commonly used in restoration works [1].

3. – Analysis methods

μ -Raman spectroscopy. – Analyses were carried out with a Senterra dispersive μ -Raman spectrometer (Bruker) using 785 nm laser source (NIR Diodes). The instrument is equipped with a Peltier-cooled CCD detector (1024×256 pixels; -70°C) and is coupled to an Olympus BX51 microscope. All spectra were collected through a $20\times$ objective, that focuses the laser in a spot size of $3 \mu\text{m}$ of diameter approximately. The power at the sample and the exposure time ranged between 50–100 mW and 100–200 s, respectively. The spectral resolution is about $3\text{--}5 \text{ cm}^{-1}$ (1200 grooves/mm gratings).

Portable FTIR (pFTIR). – FTIR analyses were performed with a portable ALPHA-R spectrometer (Bruker Optik GmbH), equipped with a cube mirror interferometer, a reflectance head with specular optics and long working distance (about 2 cm). The detector works at room temperature and the investigated spot is circular with a diameter of about 6 mm. The spectral range covered by the instrument is $350\text{--}7500 \text{ cm}^{-1}$ with 4 cm^{-1} spectral resolution. The spectra were acquired only in the $350\text{--}6000 \text{ cm}^{-1}$ range and the obvious procedure for their interpretation is to apply the well known Kramers-Kronig (KK) transformation in order to achieve the absorption spectrum to be compared with those of the reference materials.

Neutron radiography. – Neutron radiographies were performed at the ISIS neutron source. In the present case, radiographies were collected at the ROTAX station where a beam with a flux of $\sim 2 \times 10^6 \text{ s}^{-1} \text{ cm}^{-2}$ thermal neutrons covering a $\sim 3 \times 3 \text{ cm}^2$ area is available. The radiography set-up was made of a $100 \mu\text{m}$ thick $^6\text{LiF/ZnS}$ scintillator as neutron-to-light converter coupled to a Peltier-cooled CCD (Andor iStar DH712, 512×512 pixels) as image sensor [21]. Images were obtained by using a 135 mm lens, corresponding to a $\sim 5 \times 5 \text{ cm}^2$ field of view. In order to minimize blurring from the finite neutron source size, each sample was placed in contact with the outer scintillator face.

Images were processed through the IMAGEJ 1.47t package: 16-bit grey levels (corresponding to the different neutron-absorption values in different spots of the sample) were transformed in the corresponding numerical values (0 being maximum absorption and 65535 minimum absorption in the sample).

4. – Results and discussion

Micro-Raman mapping applied to polished cross sections of plasters treated with conservation products turns out to be an innovative and powerful tool for assessing their

diffusion inside the porous substrate. The behaviour of ammonium oxalate applied to painted plasters has been studied, with an immediate consequence for the conservation works, in particular concerning the treatment methodology and the influence of the plaster nature [6, 7].

Figure 1 shows an actual specimen from a mural painting treated with ammonium oxalate; the painted layer consists of red ochre pigment spread in a magnesium lime binder with an average thickness of $100\ \mu\text{m}$. The plaster is made of a magnesium lime binder as well and a silicatic aggregate with a diameter ranging from $50\ \mu\text{m}$ to $300\ \mu\text{m}$. Micro-Raman mapping allowed to define the distribution of the phases from the surface to the inner domains of the samples: the reaction of ammonium oxalate with the substrate has been ascertained by the occurrence of the C-O stretching bands of whewellite ($\text{CaC}_2\text{O}_4 \cdot \text{H}_2\text{O}$) and glunshinskite ($\text{MgC}_2\text{O}_4 \cdot 2\text{H}_2\text{O}$) [22]. The latter is the result of the ammonium oxalate reaction with the binder component rich in magnesium. Calcite and dolomite, ascribed to the binder, and gypsum, a decay product, have been detected as well (fig. 2). As shown in fig. 1 the penetration depth of the treatment ranges approximately from $80\ \mu\text{m}$ to $200\ \mu\text{m}$; in fact whewellite and glunshinskite have been detected up to this depth. Such data have a great relevance for the restoration works, even though it is destructive and it only gives point-like information. However, the overview of the ammonium oxalate diffusion has been provided by neutron techniques applied to stone specimens; the comparison of the neutron radiography of a treated (N1) and an untreated (N2) specimen highlights a strong difference: in the treated sample a noticeable absorption on the edges and a smooth absorption decrease towards the inner portion are detected (fig. 3). The radiography shows that the diffusion of the product is quite homogeneous along the entire surface reaching shallow depths (a few hundreds μm). In fig. 4 the grey scale along a line perpendicular to the edge of the two samples is plotted. The curve from the treated stone shows lower (*i.e.* darker) grey values than those of the untreated sample curve. Moreover, two absorption dips occur at the edge portions. In order to support the radiography results, μ -Raman spectra were acquired in different points along the edges. The spectroscopic findings confirm that the darker areas are really involved in the treatment: signatures of calcium oxalate (whewellite) are observed, mainly in the O-C-O stretching region (1463 and $1487\ \text{cm}^{-1}$), together with those of the CO stretching of the substrate calcite.

As a second step, neutron radiography was used to shed some light on the diffusion of organic products commonly used in the conservation sites. Different amounts of Silres BS290 were applied on the surface of plaster specimens and the neutron radiographies were compared (fig. 5). The specimen treated with $66\ \text{mg}/\text{cm}^2$ of product (S1) shows a strong absorption in the sample surface due to the occurrence of Silres BS290 (fig. 5, left), as confirmed by FTIR measurements (fig. 6e-f). The distribution of the product is poorly homogeneous and the penetration achieves different depths. The same product applied in a lower amount (S2) does not reveal any evidence of the product absorption (fig. 5, right). The detection limit of the system affects the results namely Silres BS290 is not visible at low concentrations.

Finally, neutron radiographies obtained on samples treated with Silres BS290, Paraloid B72 and Mowilith 50 at the same low concentration ($14\ \text{mg}/\text{cm}^2$) were compared. Differently from Silres BS290, the distribution of Paraloid B72 and Mowilith 50 is clearly visible on the sample surface as a homogeneous layer (fig. 7). Considering the solvents which have been used and the different properties of these compounds (such as viscosity and polymerization reaction), it is reasonable to infer that the low amount of Silres BS290 is dispersed into the matrix and it is unlikely visible in the neutron radiography.

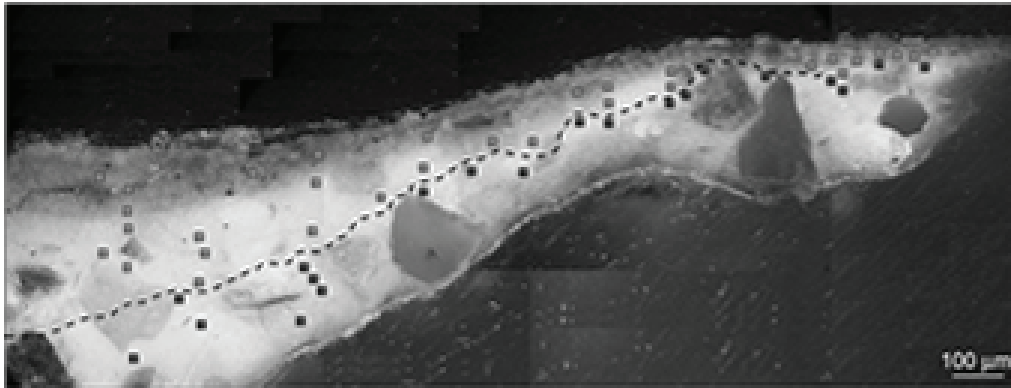


Fig. 1. – Optical image of the RC cross section with μ Raman mapping results: grey and black boxes indicate the occurrence or the absence of oxalates, respectively, thus the dashed line marks the depth achieved by the treatment.

Paraloid B72 and Mowilith 50 films observed in their radiography images are analysed with FTIR spectroscopy that confirms the reliability of the neutron technique (fig. 6a-d).

5. – Conclusions

The coupling of spectroscopy techniques and neutron radiography turns out to be an effective integrated approach for the investigation of a tricky issue in conservation field, namely the diffusion of organic-polymeric or inorganic-mineral products on the surface and inside stone materials. Advantages and disadvantages of these analytical techniques were highlighted; neutron radiography allows obtaining, in a non-destructive way, the overview of the treatment diffusion also in the case of inorganic compounds.

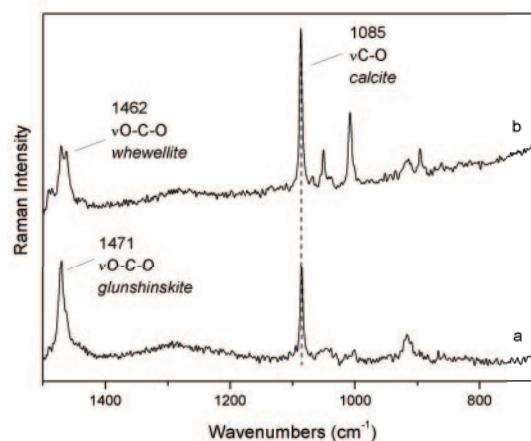


Fig. 2. – Raman spectra acquired in the RC specimen. Glunshinskite (a) and whewellite (b) confirmed the reaction between the ammonium oxalate and the calcite of the substrate (see [22] for reference spectra).

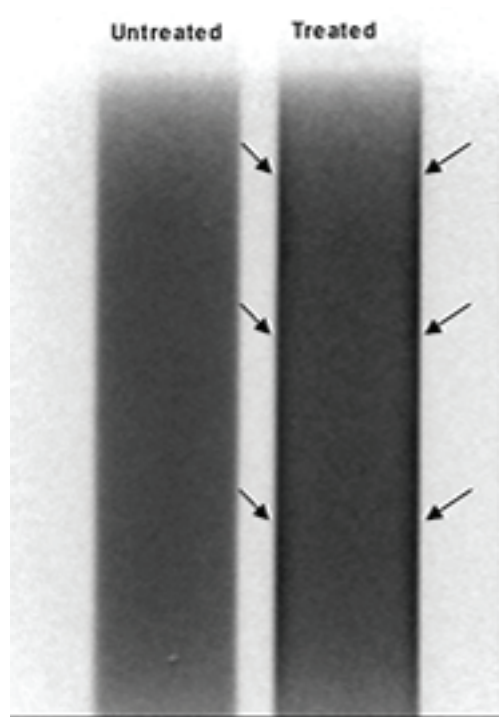


Fig. 3. – Neutron radiographies of N2 (left) and N1 (right) samples. Black arrows mark the two treated edges in which the absorption is higher.

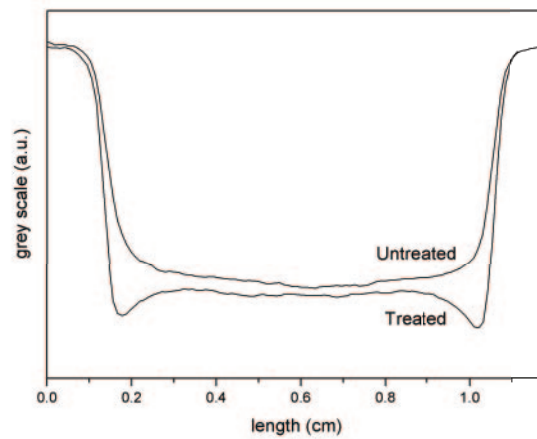


Fig. 4. – Curves of the grey scale along the line perpendicular to the edge of the specimens N1 (treated) and N2 (untreated). Note the two absorption dips occurring at the edge of the treated specimen.

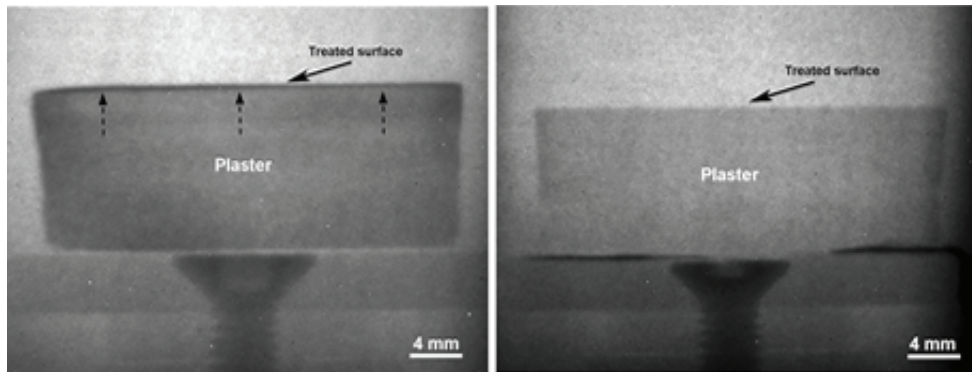


Fig. 5. – Neutron radiography of S1 (left) and S2 (right) specimens. Note the strong absorption in the surface of S1 (marked by the dashed arrows) due to the occurrence of the product and the lack of absorption in S2 specimen.

The results permit to compare the behaviour of different conservation products and also to evaluate different application methods in order to obtain the widest diffusion. On the other hand, spectroscopic techniques turn out to be essential for the identification of the product and its transformation mechanisms, as well as for a correct interpretation and full exploitation of neutron radiographies. This study provides new knowledge on the interaction between the product and the matrix and the transfer to the conservation sites of the obtained results allows the optimization of the treatments. New experiments are

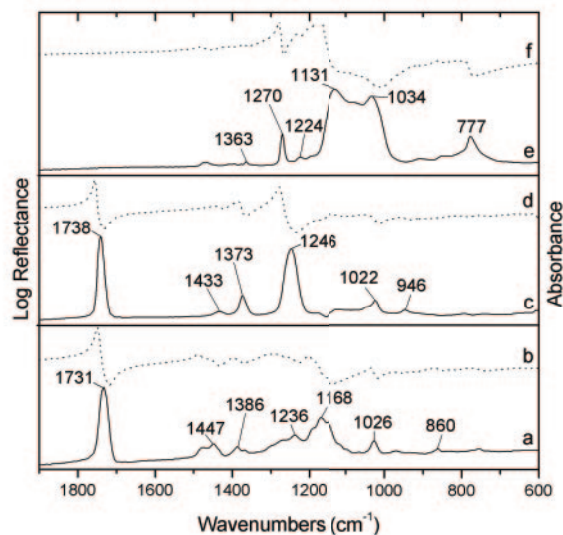


Fig. 6. – IR reflectance spectra acquired with portable instrument on the surface of the specimens before (dotted lines) and after (continuous line) KKT transformation; PB (a-b), MW (c-d) [23], S1 (e-f). Spectra a, c and e are ascribable to Paraloid B72, Mowilith 50 and Silres BS290, respectively (see [24,25] for reference spectra).

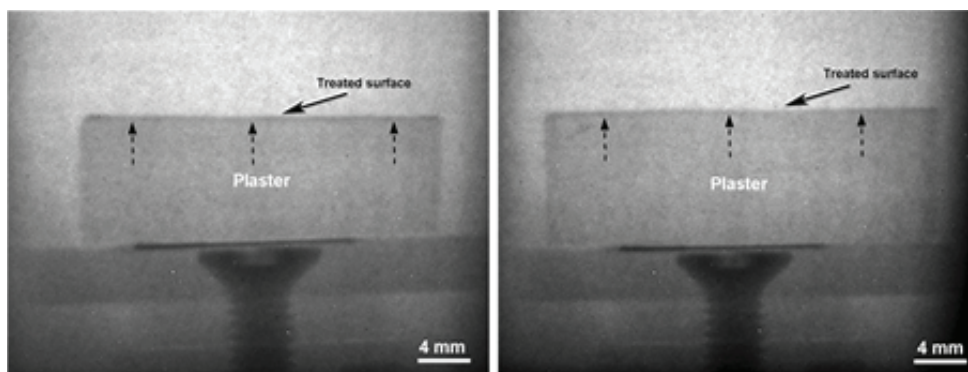


Fig. 7. – Neutron radiography of PB (left) and of MW (right) specimens. The dashed arrows mark the specimen portions with a higher neutron absorption, ascribed to the product.

in progress to improve the sensibility of the neutron radiography system thus allowing to observe smaller quantity of product distributed in a few tens of μm .

* * *

The Funding Agreement No. 06/20018 between CNR and STFC, concerning collaboration in mutual scientific research at the spallation neutron source ISIS (UK) is gratefully acknowledged. Experiments at the ISIS Pulsed Neutron and Muon Source were supported by a beamtime allocation from the Science and Technology Facilities Council.

REFERENCES

- [1] CASADIO F. and TONIOLO L. J., *Am. Inst. Conserv.*, **43** (2004) 1.
- [2] DE BUERGO M. A., FORT R. and GOMEZ-HERAS M., *Scanning*, **26** (2004) 41.
- [3] BALLESTER M. A. D. and GONZALEZ R. F., *Prog. Org. Coat.*, **43** (2001) 258.
- [4] DELGADO RODRIGUES J., FERREIRA PINTO A. and RODRIGUES DA COSTA D., *J. Cult. Her.*, **3** (2002) 117.
- [5] CADOT-LEROUX L., VERGE`S-BELMIN V., COSTA D., DELGADO RODRIGUES J., TIANO P., SNETHLAGE R., SINGER B., MASSEY S. and DE WITTE E., in *Proceedings of the Ninth International Congress on Deterioration and Conservation of Stone* (Elsevier, Amsterdam) 2000, pp. 361–369.
- [6] CONTI C., COLOMBO C., DELLASEGA D., MATTEINI M., REALINI M. and ZERBI G., *J. Cult. Her.*, **12** (2011) 372.
- [7] CONTI C., COLOMBO C., MATTEINI M., REALINI M. and ZERBI G., *J. Raman Spectrosc.*, **41** (2010) 1254.
- [8] CNUUDE V., CNUUDE J. P., DUPUIS C. and JACOBSA P. J. S., *Mater. Charact.*, **53** (2004) 259.
- [9] CNUUDE V., DIERICK M., VLASSENBOECK J., MASSCHAELE B., LEHMANN E., JACOBS P. and VAN HOOREBEKE L., *J. Cult. Her.*, **8** (2007) 331.
- [10] LEHMANN E. H., VONTOBELA P., DESCHLER-ERBB E. and SOARESC M., *Nucl. Instrum. Methods A*, **542** (2005) 68.
- [11] LEHMANN E. H., HARTMANN S. and SPEIDEL M. O., *Archaeometry*, **52** (2010) 416.
- [12] RANTA J., MILIC Z., ISTENIC J., KNIFIC T., LENGAR I. and RANT A., *Appl. Radiat. Isot.*, **64** (2006) 7.

- [13] VAN LANGH R., JAMES J., BURCA G., KOCKELMANN W., YAN ZHANG S., LEHMANN E., ESTERMANNE M. and PAPPOT A., *J. Anal. At. Spectrom.*, **26** (2011) 949.
- [14] CNUUDE V., DIERICK M., VLASSENBROECK J., MASSCHAELE B., LEHMANN E., JACOBS P. and VAN HOOREBEKE L., *Nucl. Instrum. Methods Phys. Res. B*, **266** (2008) 155.
- [15] EL ABD A., CZACHOR A. and MILCZAREK J., *Appl. Radiat. Isot.*, **67** (2009) 556.
- [16] HASSANEIN R., MEYER H. O., CARMINATI A., ESTERMANN M., LEHMANN E. and VONTOBEL P., *J. Phys. D: Appl. Phys.*, **39** (2006) 4284.
- [17] LEHMANN E., HARTMANNA S. and WYERB P., *Nucl. Instrum. Methods Phys. Res. A*, **542** (2005) 87.
- [18] HAMEED F., SCHILLINGER B., ROHATSCH A., ZAWISKY M. and RAUCH H., *Nucl. Instrum. Methods Phys. Res. A*, **605** (2009) 150.
- [19] TRIOLO R., GIAMBONA G., LO CELSO F., RUFFO I., KARDJILOV N, HILGER A., MANKE I. and PAULKE A., *Conserv. Sci. Cult. Her.*, **10** (2010) 143.
- [20] DOHERTY B., PAMPLONA M., SELVAGGI R., MILIANI C., MATTEINI M., SGAMELLOTTI A. and BRUNETTI B., *Appl. Surf. Sci.*, **253** (2007) 4477.
- [21] FINOCCHIARO V., ALIOTTA F., TRESOLDI D., PONTERIO R. C., VASI C. S. and SALVATO G., *Rev. Sci. Instrum.*, **84** (2013) 093701.
- [22] FROST R. L. and WEIER M. L., *J. Raman Spectrosc.*, **34** (2003) 776.
- [23] CHÉRCOLES ASENSIO R., SAN ANDRÉS MOYA M., DE LA ROJA J. M. and GOMEZ M., *Anal. Bioanal. Chem.*, **380** (2009) 2081.
- [24] LI X. and KING T. A., *J. Non-Cryst. Solids*, **204** (1996) 235.
- [25] JUNG H. Y., GUPTA R. K., OH EO., KIM Y. H. and WHANG C. M., *J. Non-Cryst. Solids*, **351** (2005) 372.